

University of Groningen

Hooked on mushrooms

Sharma, Preeti; Saggiomo, Vittorio; Van Der Doef, Vincent; Kamperman, Marleen; A. Dijkstra, Joshua

Published in:
 Biointerphases

DOI:
[10.1116/6.0000634](https://doi.org/10.1116/6.0000634)

IMPORTANT NOTE: You are advised to consult the publisher's version (publisher's PDF) if you wish to cite from it. Please check the document version below.

Document Version
 Publisher's PDF, also known as Version of record

Publication date:
 2021

[Link to publication in University of Groningen/UMCG research database](#)

Citation for published version (APA):

Sharma, P., Saggiomo, V., Van Der Doef, V., Kamperman, M., & A. Dijkstra, J. (2021). Hooked on mushrooms: Preparation and mechanics of a bioinspired soft probabilistic fastener. *Biointerphases*, 16(1), [011002]. <https://doi.org/10.1116/6.0000634>

Copyright

Other than for strictly personal use, it is not permitted to download or to forward/distribute the text or part of it without the consent of the author(s) and/or copyright holder(s), unless the work is under an open content license (like Creative Commons).

The publication may also be distributed here under the terms of Article 25fa of the Dutch Copyright Act, indicated by the "Taverne" license. More information can be found on the University of Groningen website: <https://www.rug.nl/library/open-access/self-archiving-pure/taverne-amendment>.

Take-down policy

If you believe that this document breaches copyright please contact us providing details, and we will remove access to the work immediately and investigate your claim.

Downloaded from the University of Groningen/UMCG research database (Pure): <http://www.rug.nl/research/portal>. For technical reasons the number of authors shown on this cover page is limited to 10 maximum.

Hooked on mushrooms: Preparation and mechanics of a bioinspired soft probabilistic fastener


Cite as: Biointerphases **16**, 011002 (2021); <https://doi.org/10.1116/6.0000634>

Submitted: 15 September 2020 • Accepted: 30 November 2020 • Published Online: 19 January 2021

 Preeti Sharma,  Vittorio Saggiomo, Vincent van der Doef, et al.

COLLECTIONS

Paper published as part of the special topic on [Special Topic Collection: Biomimetics of Biointerfaces](#)

 This paper was selected as Featured



View Online



Export Citation



CrossMark

ARTICLES YOU MAY BE INTERESTED IN

[Effect of ambient temperature on respiratory tract cells exposed to SARS-CoV-2 viral mimicking nanospheres—An experimental study](#)

Biointerphases **16**, 011006 (2021); <https://doi.org/10.1116/6.0000743>

[On formation of dry spots in heated liquid films](#)

Physics of Fluids **33**, 023601 (2021); <https://doi.org/10.1063/5.0035547>

[A perovskite retinomorphic sensor](#)

Applied Physics Letters **117**, 233501 (2020); <https://doi.org/10.1063/5.0030097>



Advance your science and
career as a member of

AVS

LEARN MORE



Hooked on mushrooms: Preparation and mechanics of a bioinspired soft probabilistic fastener

Cite as: *Biointerphases* **16**, 011002 (2021); doi: [10.1116/6.0000634](https://doi.org/10.1116/6.0000634)

Submitted: 15 September 2020 · Accepted: 30 November 2020 ·

Published Online: 19 January 2021



View Online



Export Citation



CrossMark

Preeti Sharma,^{1,a)}  Vittorio Saggiomo,²  Vincent van der Doef,¹ Marleen Kamperman,³ 
and Joshua A. Dijkman^{1,a)} 

AFFILIATIONS

¹Physical Chemistry and Soft Matter, Wageningen University & Research, Wageningen 6708 WE, Netherlands

²BioNano Technology, Wageningen University & Research, Wageningen 6700 EK, Netherlands

³Polymer Science, Zernike Institute for Advanced Materials, University of Groningen, Groningen 9747 AG, Netherlands

Note: This paper is part of the *Biointerphases* Special Topic Collection on Biomimetics of Biointerfaces.

a) Authors to whom correspondence should be addressed: preeti.sharma@wur.nl and joshua.dijkman@wur.nl

ABSTRACT

Probabilistic fasteners are known to provide strong attachment onto their respective surfaces. Examples are Velcro® and the “3M dual lock” system. However, these systems typically only function using specific counter surfaces and are often destructive to other surfaces such as fabrics. Moreover, the design parameters to optimize their functionality are not obvious. Here, we present a surface patterned with soft micrometric features inspired by the mushroom shape showing a nondestructive mechanical interlocking and thus attachment to fabrics. We provide a scalable experimental approach to prepare these surfaces and quantify the attachment strength with rheometric and video-based analysis. In these “probabilistic fasteners,” we find that higher feature densities result in higher attachment force; however, the individual feature strength is higher on a low feature density surface. We interpret our results via a load-sharing principle common in fiber bundle models. Our work provides new handles for tuning the mechanical attachment properties of soft patterned surfaces that can be used in various applications including soft robotics.

Published under license by AVS. <https://doi.org/10.1116/6.0000634>

I. INTRODUCTION

Attachment via mechanical interlocking of three-dimensional (3D) protruded features is of importance for many species in nature.¹ For instance, the arresting system in the head and wings of a dragonfly is found to effectively protect its slim neck [see Fig. 1(a) adapted from Jiao *et al.*²]. Also, many other fixation systems in numerous species such as wasps, bees, bugs, and beetles have been developed to securely attach their wings to the body while at rest.³ In the plant world, climbing of the Gallium Aparine plant works via ratchetlike attachment mechanism using micro-macroscopic hooks onto the host plant to seek more sunlight.^{4–6} Inspired by such attachment systems found in nature, smart surfaces consisting micrometer-millimetric sized attachment features are being developed for many applications such as climbing robots⁷ and grippers.⁸ The invention of Velcro® was originally inspired by

burdock seeds,⁹ and the related “3M dual lock” system¹⁰ has been successful for their applications in textile industries and medical fields. However, despite providing high attachment forces to their respective opposing surfaces, detachment of these mechanical fasteners leaves damage if attached to a fabric.

The essential problem in mechanical attachment is that the interlocking features are rigid, limiting the ability for safe removal without damaging the interlocking features or the fabric itself, also seen in the work from Fiorello *et al.*,¹¹ where plant-inspired interlocking microstructures having 3D hook shape were tested for their attachment on fabric. Another recent study by Fiorello *et al.* shows that, if a shear force parallel to the surface was applied, the interlocked features detach without producing damage on different fabrics.⁷ Surface directionality can thus resolve the damage issue, yet also limits the applicability of the attachment device.

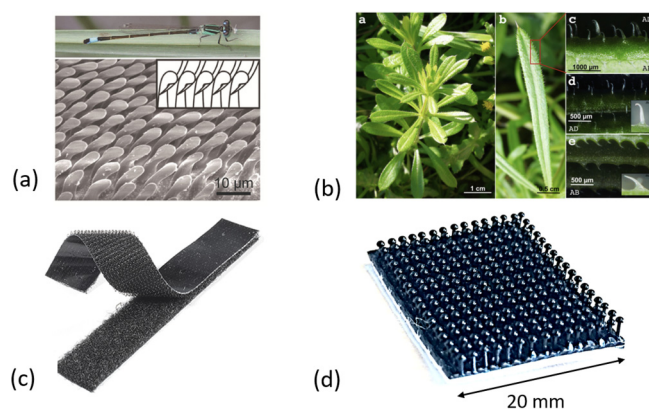


FIG. 1. Examples of natural and man-made interlocking systems. (a) Optical image of a dragonfly and microfeatures responsible for arresting mechanism in head and wings. Reproduced with permission from Jiao *et al.*, *Adv. Sci.* **5**, 1700787 (2018). Copyright 2018, John Wiley and Sons (Ref. 2). (b) Image of the herbaceous climbing plant Gallium Aparine and details of leaf and details of interlocking features in zoomed images. Reproduced with permission from Fiorello *et al.*, *Rose-Inspired Micro-device with Variable Stiffness for Remotely Controlled Release of Objects in Robotics* (Springer, Cham, 2019), pp. 122–133. Copyright 2018, Springer Nature (Ref. 14). (c) A picture of Velcro® and (d) a picture of the 3M dual lock taken from camera.

Geometries other than plant-inspired hooks such as pestle, mushroom, and Velcro hooks have also been explored for their attachment to fabrics. It was found that pestle shapes were creating the least damage onto the features and lint of fabric, but with weaker detachment force in normal direction compared to other geometries.² It is clear that having features with overhangs such as a mushroom shape or Velcro hooks are required to enhance attachment strength normal to the surface; however, the stiffness of the features results in partial or permanent damage of the interlocking features or the fabric itself. Having soft patterned surfaces with soft interlocking features would thus be an innovative step toward a new class of damage and residue-free dry adhesives that can actually attach to fabrics of different mesh sizes and potentially even to other surfaces with micro- to macroscopic roughness.

In this work, we present a soft surface, functionalized with soft micrometric mushroom-shaped features, providing mechanical interlocking, while leaving no damage on attachment features or the surface it attaches to. We describe a scalable production mechanism by combining simple 3D printing and soft lithography to achieve microscopic patterns in a soft polymer. Subsequently, we show that the surface patterns have the desired mechanical functionality; specifically, the surfaces attach to three different types of fabrics having regular and irregular mesh sizes. The soft features do not damage the fabrics, even though the attachment is based on mechanical interlocking. Apart from assuring safe detachment, we provide insight into the design parameters of the attachment mechanism by probing the interaction between the attachment features. We provide a detailed perspective for tuning the attachment strength of a soft probabilistic fastener via load-sharing rules known from rupture theory in fiber bundle models.^{12,13}

II. MATERIALS AND METHOD

A. Fabrication of microscopic patterned surfaces

Conventional lithography techniques are known for being able to create microscopic patterned surfaces in soft elastomers, indeed with high resolution, including complex 3D structures such as mushrooms having a flat disk shape hat.^{15–18} Realizing micrometric mushroom features having spherical-like shapes such as “3M dual lock” or a half-spherical hat that is essential for mechanical interlocking has not been possible below a millimeter scale. At present, 3D printers allow an easy and direct realization of complex 3D features such as microfeatures inspired by rose prickles¹⁴ and *Salvinia Molesta*.¹⁹ We have printed surfaces patterned with 3D mushroom features having spherical hats using a stereolithography 3D printer. The capability of a 3D printer to print a variety of features other than mushroom as small as 200 μm is given in Sec. 1 in the supplementary material.³³ A picture of a 3D printed sample having mushroom features can be seen in Fig. 2. The samples have been designed in a 3D computer-aided design (CAD) software (SOLIDWORKS 2017), CAD files are attached in the supplementary material.³³ The geometrical details of the features in 3D CAD and the 3D printed outcome are illustrated in Table I. The microfabricated features are in good agreement with the CAD designs for their dimensions and shape.

The cured resin from the 3D printer is a stiff material with Young’s modulus of 2.8 GPa.²⁰ Attachment and subsequent detachment from an opposing surface such as a fabric can break either the small 3D printed features or damage the fabric itself. Therefore, we replicated the 3D printed structure in polydimethylsiloxane elastomer (PDMS) using a double molding process.^{21–23} First, the positive 3D printed structure was replicated as negative in an elastomer ecoflex 0030. Afterward, PDMS Sylgard 184 was cast and cured in the negative ecoflex for making the 3D printed replica (see Fig. 2 and Sec. 3 in the supplementary material³³). Young’s modulus of the PDMS Sylgard was about 1.8 MPa for a mixing ratio of 1:10 and a curing temperature of 70°C.²⁴

We found that the alternative method of first 3D printing the negative mold and then casting the PDMS on it does not work for two reasons: printing negative molds having complex 3D features is technically not possible with the printers used, and small features on the PDMS tend to detach while peeling it off the 3D printed mold. Therefore, using double molding is necessary. Ecoflex is equally important, as it is a softer elastomer than PDMS and can be elongated to more than 900% of its original size, allowing easy demolding of the PDMS. This process results in similar 3D printed features as shown in Fig. 2(b) with shrinkage of less than 2%.²⁵

Another important aspect to take into account is the chemical composition of the different materials and the chemical reaction involved in the process. In fact, 3D printer resins are usually composed of methacrylates, which are reactive with the vinyl-terminated siloxanes present both in the ecoflex and PDMS. This means that if the 3D printed structure is not completely cured, it will react with the uncured ecoflex and it will chemically bond to it, making the peeling off impossible. Similar considerations are relevant when casting PDMS on ecoflex.²³ If the latter is not

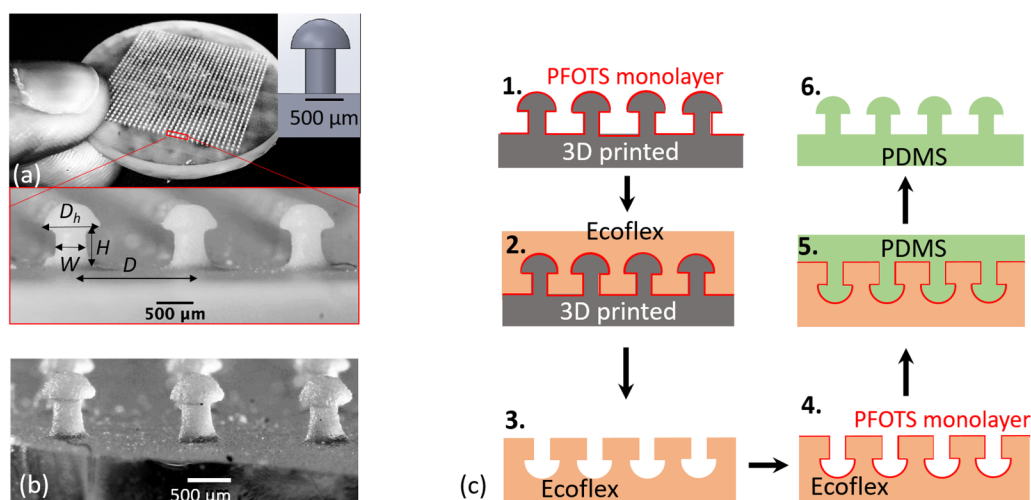


FIG. 2. (a) A picture of a 3D printed sample having mushroom features on it and corresponding side view of features in zoomed picture and side view from CAD model in the inset. (b) Microscope picture of the replica of the 3D printer features in PDMS. (c) Schematic illustration of double molding procedure: (1) 3D printed mold, (2) molding ecoflex on 3D printed, (3) negative mold in ecoflex, (4) monolayer deposition of PFOTS by chemical vapor deposition, (5) casting PDMS in ecoflex mold, and (6) PDMS sample.

properly cured, the two silicone based elastomers will react and seal together. We solved those issues using a chemical surface modification of the 3D printed and ecoflex mold. Both surfaces were first activated by a plasma oven and then reacted with perfluorodecyltrichlorosilane (PFOTS) using a chemical vapor deposition approach (see Sec. 2 in the supplementary material³³). In this way the entire surface, both on the 3D printed positive and the negative ecoflex were made nonreactive toward the hydrosilylation curing reaction.

B. Experimental setup and protocol

A schematic of the experimental setup to measure the pull-off force and explore the underlying mechanisms is depicted in Fig. 3(a). We used a rheometer (Anton Paar MCR 501) in the plate-plate configuration to record the force-distance curves and hence to estimate the attachment force. Note that rheometers are more typically known as instruments to measure the viscoelastic properties of liquids; here, we use this instrument for attachment force measurements generated by attachment of mushroom features because of their ability to apply an angle of rotation with a desired

TABLE I. Geometrical details of the mushroom features designed in CAD and 3D printed outcomes shown in Fig. 2(a). H is the mushroom stem height, W is the diameter of the stem, D is the periodicity of the features, and D_h is the diameter of the mushroom hat [see Fig. 2(a)].

Mushrooms	H (μm)	W (μm)	D (μm)	D_h (μm)
CAD model	600	400	1600	800
3D printed	594 ± 38	400 ± 15	1600 ± 2	766 ± 35

frequency and number of oscillations along with a known normal force. As such, they mimic the attachment procedure used in qualitative experiments in Sec. III A.

A single layer of fabric was fixed at the edges onto a glass substrate with scotch tape (see schematic in Sec. 5 in the supplementary material³³ and Fig. 3), which is then fixed at the bottom plate of the rheometer using UV curing glue (Norland product). A sample with mushroom features is fixed onto a glass substrate using plasma oxidation which is afterward fixed onto a top plate of the rheometer via a drop of UV curing glue. The glue is hardened while the sample is in contact with the counter surface at the bottom plate of the rheometer so that both of the contact surfaces are aligned with one another. Two cameras are used to record the attachment mechanism: one camera is placed under the transparent bottom plate of the rheometer and another one is observing the attachment dynamics from the side.

Four samples of identical size with varying feature densities, i.e., 25, 39, 69, and 83 mushroom/ cm^2 , have been used to test the attachment performance on a Nylon based synthetic fabric, abbreviated as SIF (stretchable irregular fabric) in this work. The protocol that has been used to measure attachment force with the rheometer consists of the steps described here and shown in Fig. 3(b). First, the sample makes an approach toward the fabric sample with a velocity $v = 500 \mu\text{m s}^{-1}$ to reach a normal force F_N . After a relaxation of 10 s, the top plate oscillates at an angular frequency f along with a given rotation angle θ for the number of cycles n . We then let the combined surfaces relax for 10 s while keeping the position of the top plate fixed. Finally, the top plate is retracted with the same velocity as in the approach step. In all experiments, the angle used for oscillatory motion θ is fixed to 10° as to best approximate the qualitative experiments demonstrated in Sec. III A.

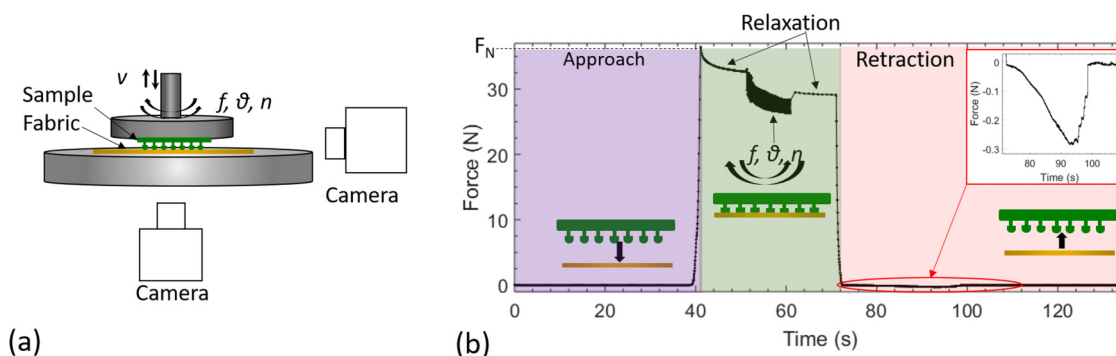


FIG. 3. (a) Schematic of the experimental setup and (b) typical force curve showing the complete experimental procedure. v is the velocity of the top plate probe during approach and retraction, f , θ , and n are the rotation frequency, angle of oscillations, and number of cycles of the top plate, respectively.

III. RESULTS AND DISCUSSIONS

A. Attachment to fabrics

At first, patterned surfaces were tested qualitatively for their attachment on three types of fabrics (Fig. 4): (1) nylon based synthetic fabric commonly known as pantyhose, which is highly stretchable in nature and has an irregular mesh size in the unstretched state. We abbreviate it as SIF in this work; (2) non-stretchable synthetic and cotton mixed fabric with a fixed mesh

size of $450 \times 750 \mu\text{m}$ called nSRF1 (nonstretchable regular fabric 1); and (3) a nonstretchable cotton fabric with a fixed mesh size of $250 \times 300 \mu\text{m}$ known as cheese-straining cloth and abbreviated as nSRF2. 3D printed samples were pressed manually against the fabric, which results in no attachment of features. To obtain mechanical interlocking of shapes with overhang in a substrate with openings, we posit that a small angular rotation with a normal pressure is essential as it allows deformation in the fabric to let the features interlock. In the case of PDMS sample, the mushroom

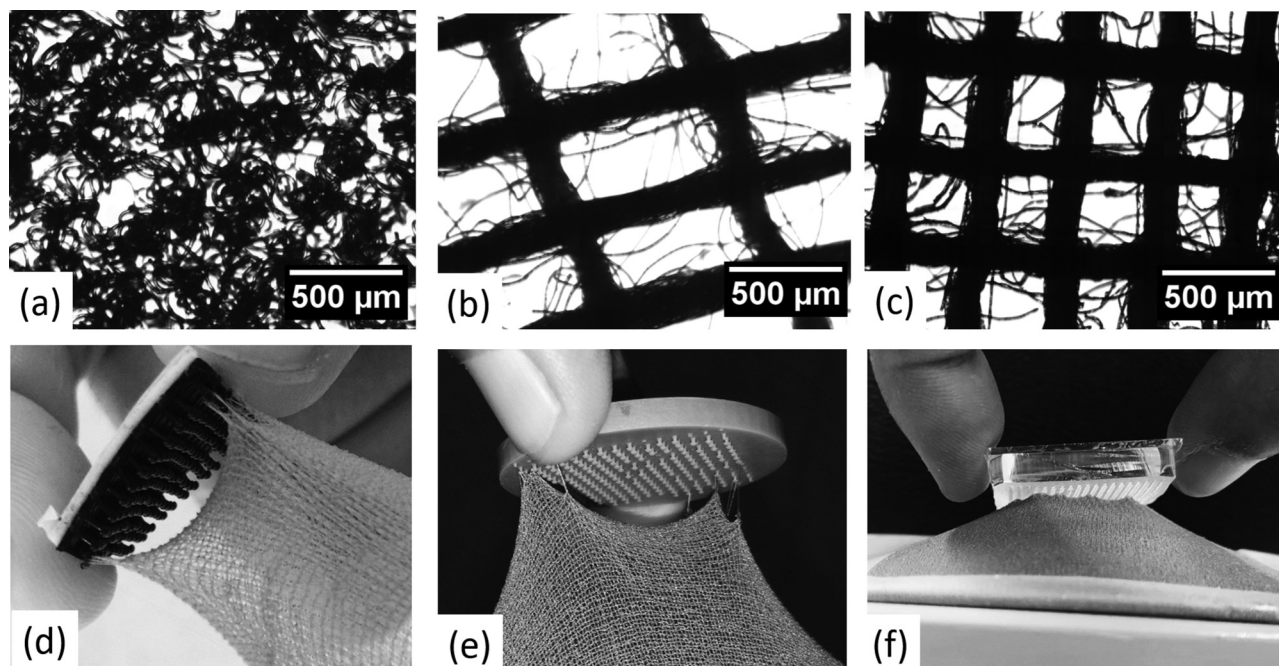


FIG. 4. Microscopic pictures of the fabrics: (a) SIF; (b) nSRF1; (c) nSRF2. Images were taken during qualitative attachment experiments of (d) 3M dual lock sample on SIF; (e) 3D printed sample having mushroom structures on SIF; and (f) PDMS sample with mushroom features onto SIF.

TABLE II. Qualitative results from the three samples on three types of textiles. ✓ denotes attachment on fabric.

Textiles	3M dual lock	3D printed sample	PDMS sample
SIF	✓, damage on fabric	✓, damage on fabric and sample	✓, no damage
nSRF1	✓, damage on fabric	✓, damage on fabric and sample	✓, no damage
nSRF2	No attachment	✓, damage on fabric and sample	✓, no damage

features also bend and the movement induces the mushroom heads to get stuck into the fabric opening (see Sec. 6 and video 1 in the supplementary material for a visual representation³³).

At first, the attachment of 3D printed sample and a piece of 3M dual lock mechanical fastener has been tested. Both samples tend to adhere to the SIF and nSRF1 fabric but at the expense of damage on the fabric as shown in Figs. 4(d) and 4(e). Also, the rupture of a few mushroom features was observed in the 3D printed sample [see Fig. 4(e)]. No damage was observed for the nSRF2 fabric as no mechanical interlocking was observed since the size of mushroom features being significantly larger than the textile mesh size. However, a sample printed with smaller mushroom features ($W = 200\mu\text{m}$, $H = 400\mu\text{m}$, $R = 200\mu\text{m}$) shows evidence of attachment to the nSRF2 fabric, but again at the expense of permanent damage on either sample or fabric. The soft mushroom sample also adheres to all fabrics. No damage was observed on fabrics or the PDMS sample itself (see Fig. 2 and Sec. 4 in the supplementary material³³). For a complete overview of attachment performance, see Table II.

B. Quantification of attachment

Figure 5(a) shows the force-displacement curves of a sample having a feature density of 39 features- cm^{-2} on SIF fabric at $F_N = 5\text{ N}$ and $f = 5\text{ Hz}$. The red curve is for $n = 0$ and black for $n = 50$. See Sec. 6 and video 2 in the supplementary material³³ to visualize the dynamics as recorded during the measurement that produced the black curve. From this experiment, it is clear that pressing is not sufficient to get the mushroom features interlocked into the fabric; hence, no attachment force was observed [see red curve (zero cycles)]. In both experiments, the retraction curve is separated from the approach curve, presumably because of some viscoelastic mechanism playing a role, perhaps due to the sliding of both the PDMS mushroom features and fabric on the glass plate. During retraction, pull-off events of varying sizes can be seen because of the subsequent detachment of a number of mushroom-fabric pairs. The peak force from this curve is used to characterize the attachment force.

First, we have optimized the oscillation frequency and number of cycles at 5 N normal force. So, we minimize the variables for a systematic study of the attachment dynamics. The attachment force initially increases linearly with the number of cycles, after which it reaches a plateau. The transition is roughly around 20 cycles,

irrespective of the frequency of oscillations. The saturation suggests that there is saturation in the number of attached features to the fabric [see Fig. 5(b)]. Clearly, the adhesive elements are interlocking on the surface; however, a visual inspection of the micrometric features is required for a better understanding of interlocking dynamics. We captured videos simultaneously with attachment experiments and detailed image analysis is given in Sec. 3 in the supplementary material.³³ The result is shown in Fig. 5(c); on the left is the outcome of the image analysis for a sample having feature density 69 features- cm^{-2} when preloaded from 10 to 35 N and, on the right, the fraction of the interlocked features to the fabric during oscillation phase is plotted against normal force at a constant oscillation frequency of 5 Hz and 50 cycles at the right. Note that the normal forces required to achieve interlocking are substantially higher than the attachment forces obtained. We attribute this to the fact that the mushrooms have to physically penetrate the fabric, making this mechanism strain dependent. The soft mushroom features compress and bend easily and in their current design need a relatively large compressive load to make their way through the fabric. Shorter mushroom stems and other geometric design features can thus be used to reduce the normal forces required.

At low normal force, a certain number of mushroom-fabric pairs are formed out of available mushroom features on the sample. Indeed, a few distinctive regions of paired mushrooms can be seen [see Fig. 5(c)], which are certainly responsible for the pull-off events seen in force-distance curves [see Fig. 5(a)]. As the normal load is increased, an expansion or creation of new paired regions occurs due to the interlocking of more features into the fabric. At a certain normal force, regions of paired mushrooms merge, and afterward, the linear increment in paired features starts to slow down reaching a saturation regime, as most of the mushrooms are already interlocked. See Fig. 5(d) where the fraction of paired mushrooms versus normal force is shown. The available features are more abundant than the actually interlocked features, as is clear from Fig. 5(c). Not all features interlock in the saturation regime as mushroom penetration is sensitive to the angular rotation. The mushroom features in the middle of the sample perceive a lower activation strain and rarely get interlocked to the fabric. Also, we can see in Fig. 5(d) that interlocking of the soft features is more obvious for the highest feature density; the presence of neighboring mushrooms stimulates mushroom penetration.

The interlocking strength of the individual features is plotted in Fig. 6(a). To clarify trends, the attachment force was normalized by the total number of paired features and is plotted against normal force per unit available features on the sample. We found that the interlocking force is higher in the case of a less dense sample, which means that the individual soft mushroom features are more strongly attached to the fabric. We attribute this to large interpillar distances, which result in less interpillar communication. This is schematically explained in the inset of Fig. 6(a), where an array of mushroom pillars is shown in the case of small and large interpillar distances. As a result of an exerted force on the pillars during detachment, it is to be expected that the backing layer deforms as well.²⁶ Depending on the interpillar distance, this deformation in the elastic matrix can couple strongly to other pillars. As a result, the lost load during the detachment of an individual pillar

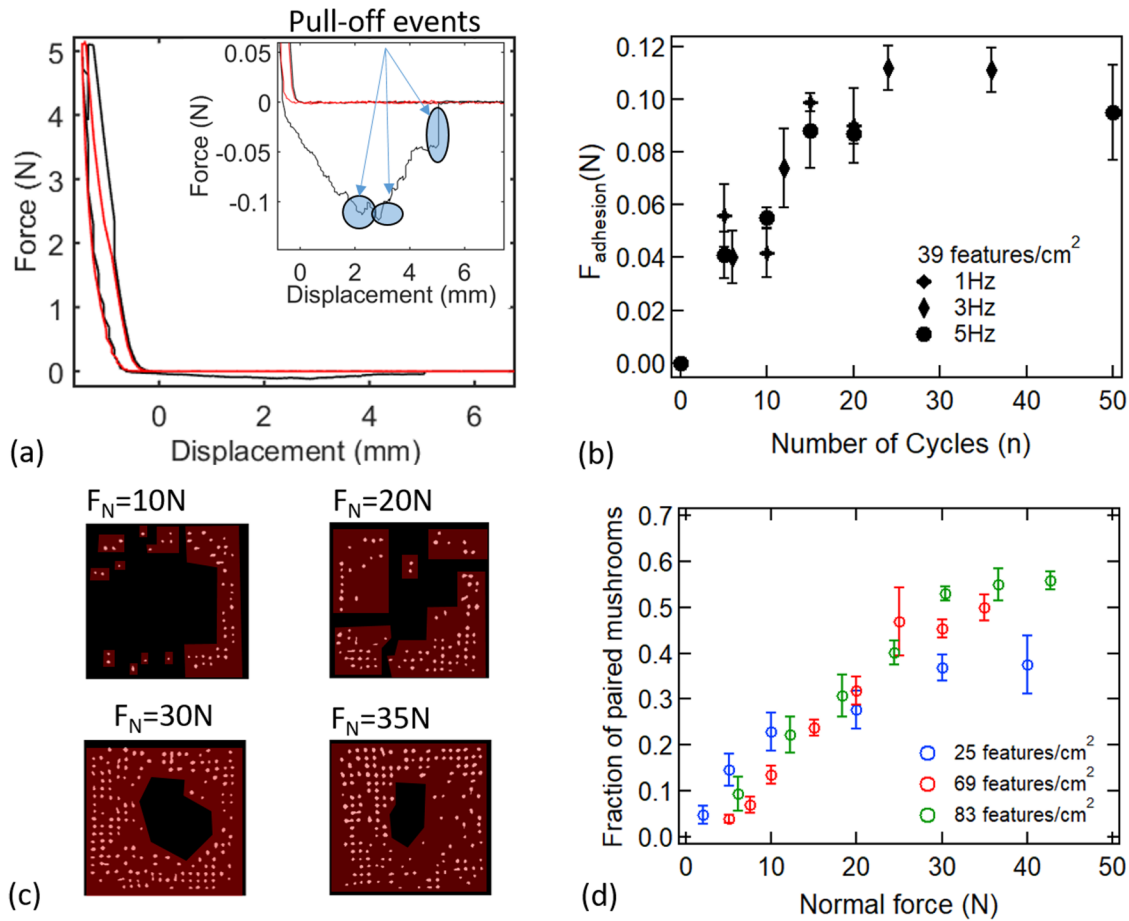


FIG. 5. (a) Force-displacement curves of mushroom sample having 39 features- cm^{-2} on SIF fabric, $v = 500 \mu\text{m/s}$, $f = 5 \text{ Hz}$, $\theta = 10^\circ$, and $n = 0$ for red and $n = 50$ for black; inset is showing the zoom of the curve during retraction. (b) Attachment force vs number of cycles at frequencies 1 Hz, 2 Hz, and 5 Hz. Normal force was 5 N. Interfacial dynamics of features: (c) result of image analysis of a sample 69 features- cm^{-2} preloaded at four different normal forces: dots are paired mushrooms to the fabric in black background and the regions of paired mushrooms are represented by the red shade and (d) fraction of interlocked mushrooms as a function of the normal force, $f = 5 \text{ Hz}$, $\theta = 10^\circ$, and $n = 50$.

is distributed locally or globally on the remaining attached features. From rupture studies in fiber bundle models, this so-called “local load-sharing” is known to lead to the catastrophic detachment of the entire paired region.^{13,27} Such effects of load-sharing have been exploited experimentally in gecko-inspired elastomeric microfibrillar adhesives, by Song *et al.*,²⁸ where the maximum adhesion force was found to be 14 times larger than the adhering membrane in local load-sharing case. We suggest that this mechanism is present in the mechanical interlocking based elastomeric adhesive as well, attributing the lower value of the individual pillar strength for samples having small interpillar distances, i.e., for with higher feature density. When the interpillar distance increases, the mushroom-fabric pair breaking follows most likely “global load-sharing” that results in a higher value of individual pillar strength during detachment as can be seen in the case of the sample having a lower feature density of 25 features/ cm^2 in Fig. 5(d).

Global load-sharing mechanics also induces another counterintuitive effect. The total adhesive strength of various samples with varying density of the features is depicted in Fig. 6(b). The attachment force increases linearly with increasing the normal force in agreement with Fig. 5(c). At a certain normal force, saturation is observed, followed by a slight decrease in force, even though there is an increase in the number of interlocking mushrooms features as recorded in Fig. 5(c). This happens due to the load-sharing effects explained in the previous paragraph: at a certain preload, a merging of regions of paired mushrooms occurs, which induces elastic coupling and hence a decrease in the detachment strength of individual interlocked mushroom with the normal force [see Fig. 6(a)]. Despite the effectiveness of global load-sharing for low asperity density surfaces, the total adhesive strength of a low asperity density surface is still lower for our particular mushroom asperity design. Having a higher

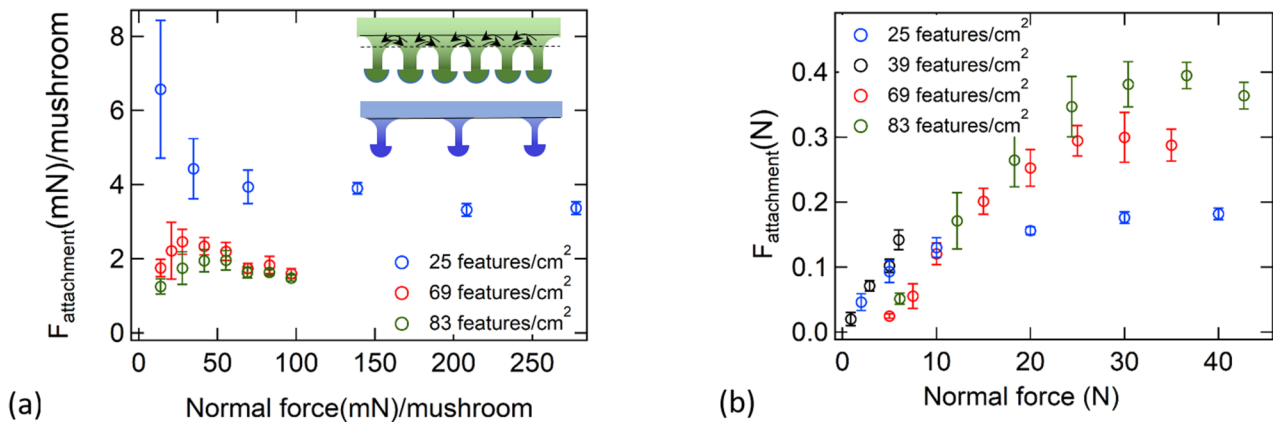


FIG. 6. (a) The interlocking force of individual paired features vs preload per unit feature; inset is a schematic illustration of increasing interpillar communication with decreasing pillar distances via the substrate deformation. (b) Attachment force vs normal force for all samples with varying feature densities, $f = 5\text{ Hz}$, $\theta = 10^\circ$, and $n = 50$.

feature density is favorable for increasing the overall attachment strength of soft mechanical adhesives simply due to the number of extra features on the surface. The dependence of the attachment strength of a patterned surface with mechanical interlocking features on the normal force has been reported in earlier works as well. In a study on plant-inspired microhooks, Fiorello *et al.*⁷ observed an increase in the detachment strength while increasing preloading force presumably more features were engaged in the interlocking mechanism. In another study of beetle-inspired wing-locking devices, Pang *et al.* observed higher detachment force due to higher overlapping of the micro-nanometric pillar.²⁹ However, to the best of our knowledge, our work is the first visual demonstration of the microscopic details of interlocking features. Also, our analysis based on load-sharing shows nontrivial scaling rules in the design of soft probabilistic fasteners. In our work, taking the fact that the highest density of the mushroom features results in the lowest attachment force per mushroom due to large elastic coupling, the maximum detachment force of soft mushrooms is $64\text{ mN}/\text{cm}^2$. This peak force is undoubtedly smaller than the work reported by Fiorello *et al.*, where the attachment of plant-inspired hooks onto polyester fabric was tested,⁷ and by Jiao *et al.*, where the pestle-loop mechanical interlocker was tested onto a knitwear fabric² (also, see Table 2 in the supplementary material³³). This is partly due to the difference in texture and mechanical properties of the studied fabrics and partly due to the stiffness of the interlocking features. The interlocking features in our work are elastic and soft: Young's modulus is approximately three orders of magnitude smaller than the literature mentioned above. Even being less stiff, the features are able to get interlock to the fabric and attributing significant attachment force without damaging the interlocking features or the fabric.

To show the adaptability of the attachment features toward a variety of fabrics with varying mesh sizes, we quantified the attachment force of one of the samples (feature density of 39

features- cm^{-2}) onto three different types of the fabrics described in Table II. The results are tabulated in Table III for their attachment forces. The force in the case of SIF is found to be smaller than in the nSRF1, even though the mesh size was larger in the case of nSRF1 fabric. The difference here is probably due to the nature of the nSRF1 fabric. Along with the mechanical interlocking of features, the nSRF1 surface allows for mechanical entanglement of some lint of the fabric around the mushroom features. This was observed directly (see video 3 and Sec. 5 in the supplementary material³³). The origin of this entanglement was the friction between the PDMS surface and fabric that generates lint. In the case of nSRF2, no mechanical interlocking of mushroom features into the mesh of fabric was observed due to the feature size being larger than the mesh size. Here, the attachment force measured comes entirely from the entanglement of the lint of fabric developed due to friction between the features and fabric (see video 4 and Sec. 6 in the supplementary material³³).

TABLE III. Summary of the measured attachment forces and related mechanisms on three types of fabrics. The error in the measured force comes from the standard deviation of three consecutive experiments.

Fabrics	Attachment force (mN)	Mechanism
SIF	142 ± 15	Mechanical interlocking of mushroom features
nSRF1	167 ± 29	Mechanical interlocking of mushroom feature, lint entanglement on mushroom features
nSRF2	60 ± 30	Lint entanglement on mushroom features

IV. CONCLUSION

We have developed soft surfaces patterned with 3D soft mushroom features. We showed how such mushroom shape features can create attachment when paired with fabrics without damaging themselves or the fabric. The attachment of mushrooms is based on interlocking; we demonstrated this by systematically changing the parameters of the custom-designed attachment application protocol. We demonstrated the effect of the feature density on the attachment strength and found that the feature distance controls detachment dynamics in a way reminiscent of fiber bundle model dynamics.

As future perspectives, we highlight that an active mechanism to minimize and/or control the elastic coupling between features can further *actively* enhance the adhesive strength of soft mechanical adhesives. The stiffness of the mushroom features or the backing layer or substrate might play a role and both can be varied in a passive or an active way.³⁰ Note that the stiffness of the PDMS polymer can be controlled passively by tuning the ratio of the curing agent mixed in the PDMS during the preparation.³¹ Also, postcuring the PDMS samples at higher temperatures affects the elastic modulus.^{24,32} Once the scaling rules for attachment force depending on the substrate stiffness are clear and actively controlled, some other design parameters such as the shape or design of the individual interlocking feature itself can be adjusted for further enhancement of the attachment strength. For instance, varying the stem length or diameter of the mushroom shape or using an arrow-shaped hat instead of a half-spherical mushroom hat are just some of the possibilities that can be explored in the future. So, our study provides a clear route toward a systematic design of soft mechanical interlocking based fasteners.

AUTHORS' CONTRIBUTIONS

P.S. and V.S. contributed equally to this work.

ACKNOWLEDGMENTS

Funding from the 4TU.Federation through the program "Soft Robotics" with Grant No. 4TU-UIT-335 is gratefully acknowledged.

DATA AVAILABILITY

The data that support the findings of this study are available from the corresponding author upon reasonable request.

REFERENCES

¹C. W. Smith, S. N. Gorb, and V. L. Popov, *Philos. Trans. R. Soc. London Ser. A* **360**, 211 (2002).
²J. Jiao, F. Zhang, T. Jiao, Z. Gu, and S. Wang, *Adv. Sci.* **5**, 1700787 (2018).
³S. N. Gorb, *Int. J. Insect Morphol. Embryol.* **27**, 205 (1998).
⁴K. J. Niklas, *Curr. Biol.* **21**, R199 (2011).
⁵G. Bauer, M.-C. Klein, S. N. Gorb, T. Speck, D. Voigt, and F. Gallenmüller, *Proc. R. Soc. B Biol. Sci.* **278**, 2233 (2011).
⁶J. Burris, S. Lenaghan, and C. Stewart, *Plant Cell Rep.* **37**, 565 (2017).

⁷I. Fiorello, O. Tricinci, G. Adele Naselli, A. Mondini, C. Filippeschi, F. Tramacere, A. Kumar Mishra, and B. Mazzolai, *Adv. Funct. Mater.* **30**, 2003380 (2020).
⁸T. Zhang, T. Liang, X. Yue, and D. Sameoto, "Integration of thermoresponsive velcro-like adhesive for soft robotic grasping of fabrics or smooth surfaces," in *2019 2nd IEEE International Conference on Soft Robotics (RoboSoft)* (IEEE, Seoul, 2019), pp. 120–125.
⁹G. de Mestral, "Velvet type fabric and method of producing same," U.S. patent US2717437A (1955).
¹⁰W. L. Melbye, N. S. K. Leigh E. Wood, M. D. Lindseth, and D. A. Bychinski, "Mushroom-type hook strip for a mechanical fastener," U.S. patent US6558602B1 (2003).
¹¹I. Fiorello, O. Tricinci, A. Kumar Mishra, F. Tramacere, C. Filippeschi, and B. Mazzolai, "Artificial system inspired by climbing mechanism of galium aparine fabricated via 3D laser lithography," in *Biomimetic and Biohybrid Systems*, edited by V. Vouloutsi, J. Halloy, A. Mura, M. Mangan, N. Lepora, T. J. Prescott, and P. F. M. J. Verschure (Springer, Cham, 2018), pp. 168–178.
¹²R. Long, C.-Y. Hui, S. Kim, and M. Sitti, *J. Appl. Phys.* **104**, 044301 (2008).
¹³Y. Mulla, G. Oliveri, J. T. B. Overvelde, and G. H. Koenderink, *Phys. Rev. Lett.* **120**, 268002 (2018).
¹⁴I. Fiorello, F. Meder, O. Tricinci, C. Filippeschi, and B. Mazzolai, *Rose-Inspired Micro-device with Variable Stiffness for Remotely Controlled Release of Objects in Robotics* (Springer, Cham, 2019), pp. 122–133.
¹⁵L. Heepe and S. Gorb, *Annu. Rev. Mater. Res.* **44**, 173 (2014).
¹⁶Y. Wang, H. H. Jinyou Shao, and Y. Ding, *ACS Appl. Mater. Interfaces* **6**, 2213 (2014).
¹⁷S. C. L. Fischer, O. Levy, E. Kroner, R. Hensel, J. M. Karp, and E. Arzt, *J. Mech. Behav. Biomed. Mater.* **61**, 87 (2016).
¹⁸M. Seong, H.-H. Park, I. Hwang, and H. Eui Jeong, *Coatings* **9**, 48 (2019).
¹⁹O. Tricinci, T. Terencio, B. Mazzolai, N. M. Pugno, F. Greco, and V. Mattoli, *ACS Appl. Mater. Interfaces* **7**, 25560 (2015).
²⁰FORMLABS, Mater. High Resolut. Rapid Prototyping, 4 (2016), see <https://formlabs-media.formlabs.com/datasheets/Standard-DataSheet.pdf>.
²¹H. G. Andrews and J. P. S. Badyal, *J. Adhes. Sci. Technol.* **28**, 1243 (2014).
²²D. Chandra and S. Yang, *Acc. Chem. Res.* **43**, 1080 (2010).
²³A. Iuliano, E. van der Wal, C. W. B. Ruijmbek, S. L. M. in 't Groen, W. W. M. Pim Pijnappel, J. C. de Greef, and V. Saggiomo, *Adv. Mater. Technol.* **5**, 2000344 (2020).
²⁴I. D. Johnston, D. K. McCluskey, C. K. L. Tan, and M. C. Tracey, *J. Micromech. Microeng.* **24**, 035017 (2014).
²⁵M. Madsen, N. Feidenhans'l, P.-E. Hansen, J. Garnæs, and K. Dirscherl, *J. Micromech. Microeng.* **24**, 127002 (2014).
²⁶I. N. Sneddon, *Int. J. Eng. Sci.* **3**, 47 (1965).
²⁷*Local and Intermediate Load Sharing*, edited by A. Hansen, P. C. Hemmer, and S. Pradhan (Wiley, Weinheim, 2015), Chap. 4, pp. 63–114.
²⁸S. Song, D.-M. Drotlef, C. Majidi, and M. Sitti, *Proc. Natl. Acad. Sci. U.S.A.* **114**, E4344 (2017).
²⁹C. Pang, D. Kang, T.-I. Kim, and K.-Y. Suh, *Langmuir* **28**, 2181 (2012).
³⁰M. Tatari, A. Mohammadi Nasab, K. T. Turner, and W. Shan, *Adv. Mater. Interfaces* **5**, 1800321 (2018).
³¹J. Yull Park, S. J. Yoo, E. Joong Lee, D. H. Lee, J. Young Kim, and S. Hoon Lee, *Biochip J.* **4**, 230 (2010).
³²M. Kim, B.-U. Moon, and C. H. Hidrovo, *J. Micromech. Microeng.* **23**, 095024 (2013).
³³See supplementary material at <http://dx.doi.org/10.1116/6.0000634> for 3D printed surfaces with variety of complex features, CAD files, recorded videos, images qualitative analysis of attachment, image analysis and table showing comparison with literature.